

# Applications of Carbon Nanotubes

Pulickel M. Ajayan<sup>1</sup> and Otto Z. Zhou<sup>2</sup>

<sup>1</sup> Department of Materials Science and Engineering  
Rensselaer Polytechnic Institute, Troy, NY 12180-3590, USA  
Ajayan@rpi.edu

<sup>2</sup> Curriculum in Applied and Materials Sciences  
Department of Physics and Astronomy  
University of North Carolina at Chapel Hill  
Chapel Hill, NC 27599-3255, USA  
Zhou@physics.unc.edu

**Abstract.** Carbon nanotubes have attracted the fancy of many scientists worldwide. The small dimensions, strength and the remarkable physical properties of these structures make them a very unique material with a whole range of promising applications. In this review we describe some of the important materials science applications of carbon nanotubes. Specifically we discuss the electronic and electrochemical applications of nanotubes, nanotubes as mechanical reinforcements in high performance composites, nanotube-based field emitters, and their use as nanoprobe in metrology and biological and chemical investigations, and as templates for the creation of other nanostructures. Electronic properties and device applications of nanotubes are treated elsewhere in the book. The challenges that ensue in realizing some of these applications are also discussed from the point of view of manufacturing, processing, and cost considerations.

The discovery of fullerenes [1] provided exciting insights into carbon nanostructures and how architectures built from  $sp^2$  carbon units based on simple geometrical principles can result in new symmetries and structures that have fascinating and useful properties. Carbon nanotubes represent the most striking example. About a decade after their discovery [2], the new knowledge available in this field indicates that nanotubes may be used in a number of practical applications. There have been great improvements in synthesis techniques, which can now produce reasonably pure nanotubes in gram quantities. Studies of structure–topology–property relations in nanotubes have been strongly supported, and in some cases preceded, by theoretical modeling that has provided insights for experimentalists into new directions and has assisted the rapid expansion of this field [3,4,5,6,7,8].

Quasi-one-dimensional carbon whiskers or nanotubes are perfectly straight tubules with diameters of nanometer size, and properties close to that of an ideal graphite fiber. Carbon nanotubes were discovered accidentally by Sumio Iijima in 1991, while studying the surfaces of graphite electrodes used in an electric arc discharge [2]. His observation and analysis of the nanotube structure started a new direction in carbon research, which complemented the excitement and activities then prevalent in fullerene research. These tiny

carbon tubes with incredible strength and fascinating electronic properties appear to be ready to overtake fullerenes in the race to the technological marketplace. It is the structure, topology and size of nanotubes that make their properties exciting compared to the parent, planar graphite-related structures, such as are for example found in carbon fibers.

The uniqueness of the nanotube arises from its structure and the inherent subtlety in the structure, which is the helicity in the arrangement of the carbon atoms in hexagonal arrays on their surface honeycomb lattices. The helicity (local symmetry), along with the diameter (which determines the size of the repeating structural unit) introduces significant changes in the electronic density of states, and hence provides a unique electronic character for the nanotubes. These novel electronic properties create a range of fascinating electronic device applications and this subject matter is discussed briefly elsewhere in this volume [9], and has been the subject of discussion in earlier reviews [8]. The other factor of importance in what determines the uniqueness in physical properties is topology, or the closed nature of individual nanotube shells; when individual layers are closed on to themselves, certain aspects of the anisotropic properties of graphite disappear, making the structure remarkably different from graphite. The combination of size, structure and topology endows nanotubes with important mechanical properties (e.g., high stability, strength and stiffness, combined with low density and elastic deformability) and with special surface properties (selectivity, surface chemistry), and the applications based on these properties form the central topic of this chapter. In addition to the helical lattice structure and closed topology, topological defects in nanotubes (five member Stone–Wales defects near the tube ends, aiding in their closure) [9,10], akin to those found in the fullerenes structures, result in local perturbations to their electronic structure [11]; for example, the ends or caps of the nanotubes are more metallic than the cylinders, due to the concentration of pentagonal defects [11]. These defects also enhance the reactivity of tube ends, giving the possibility of opening the tubes [12], functionalizing the tube ends [13], and filling the tubes with foreign substances [14,15,16].

The structure of nanotubes remains distinctly different from traditional carbon fibers that have been industrially used for several decades (e.g., as reinforcements in tennis rackets, airplane frame parts and batteries to name a few) [17,18]. Most importantly, nanotubes, for the first time represent the ideal, most perfect and ordered, carbon fiber, the structure of which is entirely known at the atomic level. It is this predictability that mainly distinguishes nanotubes from other carbon fibers and puts them along with molecular fullerene species in a special category of prototype materials. Among the nanotubes, two varieties, which differ in the arrangement of their graphene cylinders, share the limelight. Multi-Walled NanoTubes (MWNT), are collections of several concentric graphene cylinders and are larger structures compared to Single-Walled NanoTubes (SWNTs) which are individual cylinders

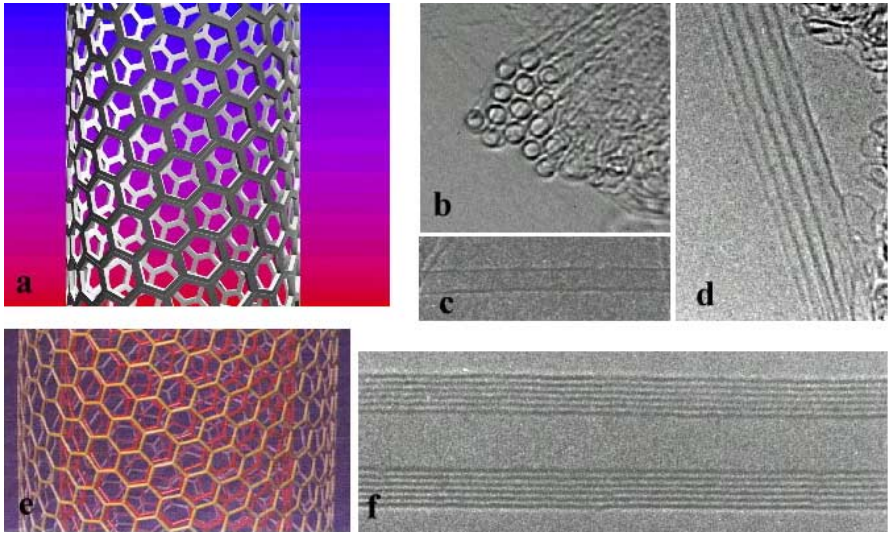


**Fig. 1.** Structure of Single-Walled (SWNT) (a-d) and Multi-Walled (MWNT) carbon NanoTubes (e,f). (a) Shows a schematic of an individual helical SWNT. (b) Shows a cross-sectional view (TEM image) of a bundle of SWNTs [transverse view shown in (d)]. Each nanotube has a diameter of  $\sim 1.4$  nm and the tube-tube distance in the bundles is 0.315 nm. (c) Shows the high-resolution TEM micrograph of a 1.5 nm diameter SWNT. (e) is the schematic of a MWNT and (f) shows a high resolution TEM image of an individual MWNT. The distance between horizontal fringes (layers of the tube) in (f) is 0.34 nm (close to the interlayer spacing in graphite)

of 1–2 nm diameter (see Fig. 1). The former can be considered as a mesoscale graphite system, whereas the latter is truly a single large molecule. However, SWNTs also show a strong tendency to bundle up into ropes, consisting of aggregates of several tens of individual tubes organized into a one-dimensional triangular lattice. One point to note is that in most applications, although the individual nanotubes should have the most appealing properties, one has to deal with the behavior of the aggregates (MWNT or SWNT ropes), as produced in actual samples. The best presently available methods to produce ideal nanotubes are based on the electric arc [19,20] and laser ablation processes [21]. The material prepared by these techniques has to be purified using chemical and separation methods. None of these techniques are scalable to make the industrial quantities needed for many applications (e.g., in composites), and this has been a bottleneck in nanotube R&D. In recent years, work has focused on developing Chemical Vapor Deposition (CVD) techniques using catalyst particles and hydrocarbon precursors to grow nanotubes [22,23,24,25]; such techniques have been used earlier to produce hollow nanofibers of carbon in large quantities [17,18]. The drawback of the catalytic CVD-based nanotube production is the inferior quality of the structures that

contain gross defects (twists, tilt boundaries etc.), particularly because the structures are created at much lower temperatures (600–1000°C) compared to the arc or laser processes ( $\sim 2000^\circ\text{C}$ ).

Since their discovery in 1991, several demonstrations have suggested potential applications of nanotubes. These include the use of nanotubes as electron field emitters for vacuum microelectronic devices, individual MWNTs and SWNTs attached to the end of an Atomic Force Microscope (AFM) tip for use as nanoprobe, MWNTs as efficient supports in heterogeneous catalysis and as microelectrodes in electrochemical reactions, and SWNTs as good media for lithium and hydrogen storage. Some of these could become real marketable applications in the near future, but others need further modification and optimization. Areas where predicted or tested nanotube properties appear to be exceptionally promising are mechanical reinforcing and electronic device applications. The lack of availability of bulk amounts of well-defined samples and the lack of knowledge about organizing and manipulating objects such as nanotubes (due to their sub-micron sizes) have hindered progress in developing these applications. The last few years, however, have seen important breakthroughs that have resulted in the availability of nearly uniform bulk samples. There still remains a strong need for better control in purifying and manipulating nanotubes, especially through generalized approaches such as chemistry. Development of functional devices/structures based on nanotubes will surely have a significant impact on future technology needs. In the following sections we describe the potential of materials science-related applications of nanotubes and the challenges that need to be overcome to reach these hefty goals.

In the following sections we describe several interesting applications of carbon nanotubes based on some of the remarkable materials properties of nanotubes. Electron field emission characteristics of nanotubes and applications based on this, nanotubes as energy storage media, the potential of nanotubes as fillers in high performance polymer and ceramic composites, nanotubes as novel probes and sensors, and the use of nanotubes for template-based synthesis of nanostructures are the major topics that are discussed in the sections that follow.

## 1 Potential Application of CNTs in Vacuum Microelectronics

Field emission is an attractive source for electrons compared to thermionic emission. It is a quantum effect. When subject to a sufficiently high electric field, electrons near the Fermi level can overcome the energy barrier to escape to the vacuum level. The basic physics of electron emission is well developed. The emission current from a metal surface is determined by the Fowler–Nordheim equation:  $I = aV^2 \exp(-b\phi^{3/2}/\beta V)$  where  $I$ ,  $V$ ,  $\phi$ ,  $\beta$ , are

the current, applied voltage, work function, and field enhancement factor, respectively [26,27].

Electron field emission materials have been investigated extensively for technological applications, such as flat panel displays, electron guns in electron microscopes, microwave amplifiers [28]. For technological applications, electron emissive materials should have low threshold emission fields and should be stable at high current density. A current density of 1–10 mA/cm<sup>2</sup> is required for displays [29] and > 500 mA/cm<sup>2</sup> for a microwave amplifier [30]. In order to minimize the electron emission threshold field, it is desirable to have emitters with a low work function and a large field enhancement factor. The work function is an intrinsic materials property. The field enhancement factor depends mostly on the geometry of the emitter and can be approximated as:  $\beta = 1/5r$  where  $r$  is the radius of the emitter tip. Processing techniques have been developed to fabricate emitters such as Spindt-type emitters, with a sub-micron tip radius [28]. However, the process is costly and the emitters have only limited lifetime. Failure is often caused by ion bombardment from the residual gas species that blunt the emission tips. Table 1 lists the threshold electrical field values for a 10 mA/cm<sup>2</sup> current density for some typical materials.

**Table 1.** Threshold electrical field values for different materials for a 10 mA/cm<sup>2</sup> current density (data taken from [31,32])

Material	Threshold electrical field (V/μm)
Mo tips	50–100
Si tips	50–100
<i>p</i> -type semiconducting diamond	130
Undoped, defective CVD diamond	30–120
Amorphous diamond	20–40
Cs-coated diamond	20–30
Graphite powder(<1 mm size)	17
Nanostructured diamond <sup>a</sup>	3–5 (unstable >30 mA/cm <sup>2</sup> )
Carbon nanotubes <sup>b</sup>	1–3 (stable at 1 A/cm <sup>2</sup> )

<sup>a</sup>Heat-treated in H plasma.

<sup>b</sup>random SWNT film

Carbon nanotubes have the right combination of properties – nanometer-size diameter, structural integrity, high electrical conductivity, and chemical stability – that make good electron emitters [27]. Electron field emission from carbon nanotubes was first demonstrated in 1995 [33], and has since been studied intensively on various carbon nanotube materials. Compared to conventional emitters, carbon nanotubes exhibit a lower threshold electric field, as illustrated in Table 1. The current-carrying capability and emission stability of the various carbon nanotubes, however, vary considerably depending on the fabrication process and synthesis conditions.

The I–V characteristics of different types of carbon nanotubes have been reported, including individual nanotubes [33,34], MWNTs embedded in epoxy matrices [35,36], MWNT films [37,38], SWNTs [39,40,41,42] and aligned MWNT films [32]. Figure 2 shows typical emission I–V characteristics measured from a random SWNT film at different anode-cathode distances, and the Fowler–Nordheim plot of the same data is shown as the inset. Turn-on and threshold fields are often used to describe the electrical field required for emission. The former is not well-defined and typically refers to the field that is required to yield 1 nA of total emission current, while the latter refers to the field required to yield a given current density, such as 10 mA/cm<sup>2</sup>. For random SWNT films, the threshold field for 10 mA/cm<sup>2</sup> is in the range of 2–3 V/μm. Random and aligned MWNTs [fabricated at the University of North Carolina (UNC) and AT&T Bell Labs] were found to have threshold fields slightly larger than that of the SWNT films and are typically in the range of 3–5 V/μm for a 10 mA/cm<sup>2</sup> current density [32] (Fig. 3). These values for the threshold field are all significantly better than those from conventional field emitters such as the Mo and Si tips which have a threshold electric field of 50–100 V/μm (Table 1). It is interesting to note that the aligned MWNT films do not perform better than the random films. This is due to the electrical screening effect arising from closely packed nanotubes [43]. The low threshold field for electron emission observed in carbon nanotubes is a direct result of the large field enhancement factor rather than a reduced electron work function. The latter was found to be 4.8 eV for SWNTs, 0.1–0.2 eV larger than that of graphite [44].

SWNTs generally have a higher degree of structural perfection than either MWNTs or CVD-grown materials and have a capability for achieving higher current densities and have a longer lifetime [32]. Stable emission above 20 mA/cm<sup>2</sup> has been demonstrated in SWNT films deposited on Si substrates [40]. A current density above 4 A/cm<sup>2</sup> (measured by a 1 mm local probe) was obtained from SWNTs produced by the laser ablation method [40]. Figure 4 is a CCD (Charge Coupled Device) image of the set-up for electron emission measurement, showing a Mo anode (1 mm diameter) and the edge of the SWNT cathode in a vacuum chamber. The Mo anode is glowing due to bombarding from field emitted electrons, demonstrating the high current capability of the SWNTs. This particular image was taken at a current density of 0.9 A/cm<sup>2</sup>. The current densities observed from the carbon nanotubes are significantly higher than from conventional emitters, such as nano-diamonds which tend to fail below 30 mA/cm<sup>2</sup> current density [31]. Carbon nanotube emitters are particularly attractive for a variety of applications including microwave amplifiers.

Although carbon nanotube emitters show clear advantageous properties over conventional emitters in terms of threshold electrical field and current density, their emission site density (number of functioning emitters per unit area) is still too low for high resolution display applications. Films presently

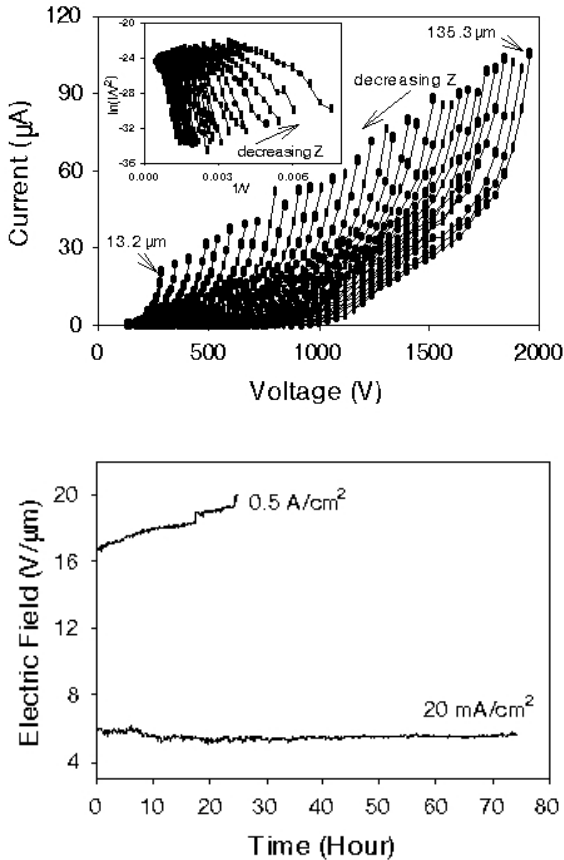


**Fig. 2.** (*Top*): Emission I–V characteristics of a random single-walled carbon nanotube film measured at different anode-cathode distances at  $10^{-8}$  torr base pressure. The same data are plotted as  $[\ln(I/V^2) \text{ vs } 1/V]$  in the *inset*. Deviations from the ideal Fowler–Nordheim behavior are observed at high current. (*Bottom*): Stability test of a random laser-ablation-grown SWNT film showing stable emission at  $20 \text{ mA/cm}^2$  (from [40])

fabricated [32] have typical emission site densities of  $10^3\text{--}10^4/\text{cm}^2$  at the turn-on field, and  $\sim 10^6/\text{cm}^2$  is typically required for high resolution display devices.

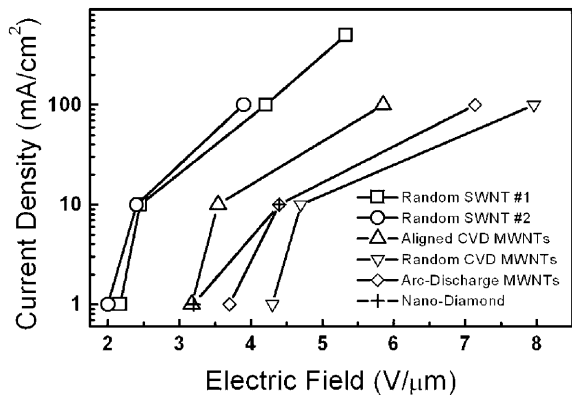


**Fig. 3.** Current density versus electric field measured for various forms of carbon nanotubes (data taken from Bower et al. [32])



**Fig. 4.** A CCD image showing a glowing Mo anode (1 mm diameter) at an emission current density of  $0.9 \text{ A/cm}^2$  from a SWNT cathode. Heating of the anode is due to field emitted electrons bombarding the Mo probe, thereby demonstrating a high current density (image provided by Dr. Wei Zhu of Bell Labs)

## 1.1 Prototype Electron Emission Devices Based on Carbon Nanotubes

### 1.1.1 Cathode-Ray Lighting Elements

Cathode ray lighting elements with carbon nanotube materials as the field emitters have been fabricated by Ise Electronic Co. in Japan [45]. As illustrated in Fig. 5, these nanotube-based lighting elements have a triode-type design. In the early models, cylindrical rods containing MWNTs, formed as a deposit by the arc-discharge method, were cut into thin disks and were glued to stainless steel plates by silver paste. In later models, nanotubes are now screen-printed onto the metal plates. A phosphor screen is printed on the inner surfaces of a glass plate. Different colors are obtained by using different fluorescent materials. The luminance of the phosphor screens measured on the tube axis is  $6.4 \times 10^4 \text{ cd/cm}^2$  for green light at an anode current of  $200 \mu\text{A}$ ,

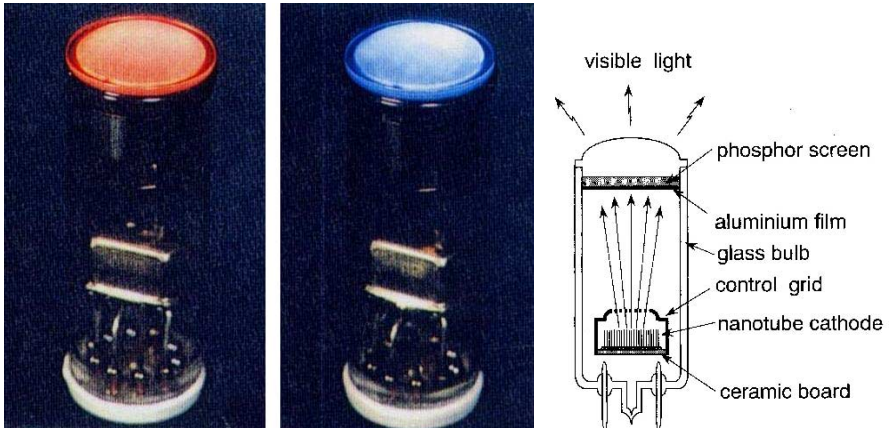


**Fig. 5.** Demonstration field emission light source using carbon nanotubes as the cathodes (fabricated by Ise Electronic Co., Japan) [45]

which is two times more intense than that of conventional thermionic Cathode Ray Tube (CRT) lighting elements operated under similar conditions [45].

### 1.1.2 Flat Panel Display

Prototype matrix-addressable diode flat panel displays have been fabricated using carbon nanotubes as the electron emission source [46]. One demonstration (demo) structure constructed at Northwestern University consists of nanotube-epoxy stripes on the cathode glass plate and phosphor-coated Indium-Tin-Oxide (ITO) stripes on the anode plate [46]. Pixels are formed at the intersection of cathode and anode stripes, as illustrated in Fig. 6. At a cathode-anode gap distance of  $30\mu\text{m}$ , 230 V is required to obtain the emission current density necessary to drive the diode display ( $\sim 76\mu\text{mA}/\text{mm}^2$ ). The device is operated using the half-voltage off-pixel scheme. Pulses of  $\pm 150\text{V}$  are switched among anode and cathode stripes, respectively to produce an image.

Recently, a 4.5 inch diode-type field emission display has been fabricated by Samsung (Fig. 6), with SWNT stripes on the cathode and phosphor-coated ITO stripes on the anode running orthogonally to the cathode stripes [47]. SWNTs synthesized by the arc-discharge method were dispersed in isopropyl alcohol and then mixed with an organic mixture of nitro cellulose. The paste was squeezed into sodalime glasses through a metal mesh,  $20\mu\text{m}$  in size, and then heat-treated to remove the organic binder.  $\text{Y}_2\text{O}_2\text{S}:\text{Eu}$ ,  $\text{ZnS}:\text{Cu,Al}$ , and  $\text{ZnS}:\text{Ag,Cl}$ , phosphor-coated glass is used as the anode.

### 1.1.3 Gas-Discharge Tubes in Telecom Networks

Gas discharge tube protectors, usually consisting of two electrodes parallel to each other in a sealed ceramic case filled with a mixture of noble gases,

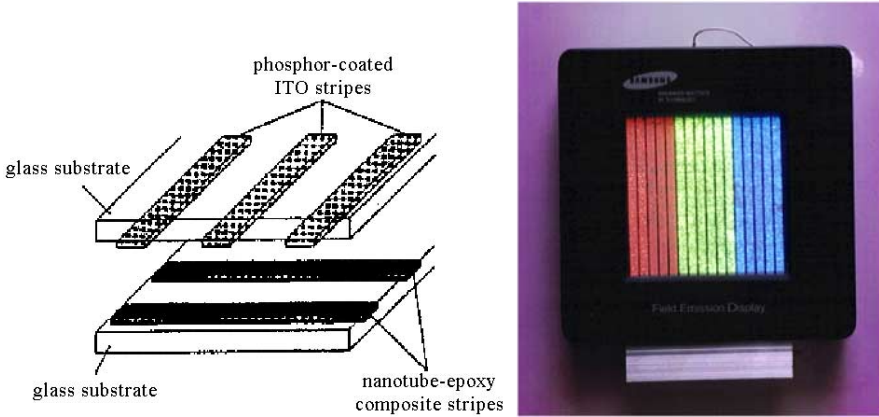


**Fig. 6.** *Left:* Schematic of a prototype field emission display using carbon nanotubes (adapted from [46]). *Right:* A prototype 4.5" field emission display fabricated by Samsung using carbon nanotubes (image provided by Dr. W. Choi of Samsung Advanced Institute of Technologies)

is one of the oldest methods used to protect against transient over-voltages in a circuit [48]. They are widely used in telecom network interface device boxes and central office switching gear to provide protection from lightning and ac power cross faults on the telecom network. They are designed to be insulating under normal voltage and current flow. Under large transient voltages, such as from lightning, a discharge is formed between the metal electrodes, creating a plasma breakdown of the noble gases inside the tube. In the plasma state, the gas tube becomes a conductor, essentially short-circuiting the system and thus protecting the electrical components from over-voltage damage. These devices are robust, moderately inexpensive, and have a relatively small shunt capacitance, so they do not limit the bandwidth of high-frequency circuits as much as other nonlinear shunt components. Compared to solid state protectors, GDTs can carry much higher currents. However, the current Gas Discharge Tube (GDT) protector units are unreliable from the standpoint of mean turn-on voltage and run-to-run variability.

Prototype GDT devices using carbon nanotube coated electrodes have recently been fabricated and tested by a group from UNC and Raychem Co. [49]. Molybdenum electrodes with various interlayer materials were coated with single-walled carbon nanotubes and analyzed for both electron field emission and discharge properties. A mean dc breakdown voltage of 448.5 V and a standard deviation of 4.8 V over 100 surges were observed in nanotube-based GDTs with 1 mm gap spacing between the electrodes. The breakdown reliability is a factor of 4–20 better and the breakdown voltage is ~30% lower than the two commercial products measured (Fig. 7). The enhanced performance shows that nanotube-based GDTs are attractive over-voltage protection units in advanced telecom networks such as an Asymmetric-Digital-Signal-Line

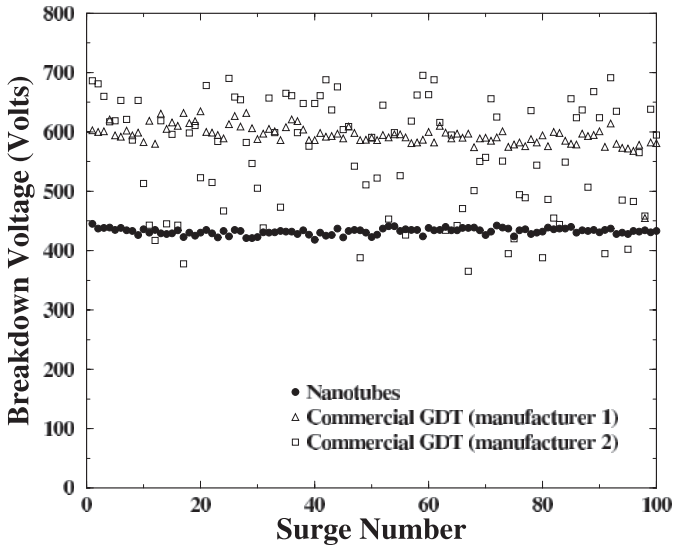


**Fig. 7.** DC breakdown voltage of a gas discharge tube with SWNT coated electrodes, filled with 15 torr argon with neon added and 1 mm distance between the electrodes. The commercial GDTs are off-the-shelf products with unknown filling gas(es), but with the same electrode-electrode gap distances. The breakdown voltage of the GDT with SWNT coated electrodes is 448.5 V, with a standard deviation of 4.8 V over 100 surges. The commercial GDT from one manufacturer has a mean breakdown voltage of 594 V and a standard deviation of 20 V. The GDT from the second manufacturer has a breakdown voltage of 563 V and a standard deviation of 93 V (from *Rosen et al.* in [49])

(ADSL), where the tolerance is narrower than what can be provided by the current commercial GDTs.

## 2 Energy Storage

Carbon nanotubes are being considered for energy production and storage. Graphite, carbonaceous materials and carbon fiber electrodes have been used for decades in fuel cells, battery and several other electrochemical applications [50]. Nanotubes are special because they have small dimensions, a smooth surface topology, and perfect surface specificity, since only the basal graphite planes are exposed in their structure. The rate of electron transfer at carbon electrodes ultimately determines the efficiency of fuel cells and this depends on various factors, such as the structure and morphology of the carbon material used in the electrodes. Several experiments have pointed out that compared to conventional carbon electrodes, the electron transfer kinetics take place fastest on nanotubes, following ideal Nernstian behavior [51]. Nanotube microelectrodes have been constructed using a binder and

have been successfully used in bioelectrochemical reactions (e.g., oxidation of dopamine). Their performance has been found to be superior to other carbon electrodes in terms of reaction rates and reversibility [52]. Pure MWNTs and MWNTs deposited with metal catalysts (Pd, Pt, Ag) have been used to electro-catalyze an oxygen reduction reaction, which is important for fuel cells [53,54,55]. It is seen from several studies that nanotubes could be excellent replacements for conventional carbon-based electrodes. Similarly, the improved selectivity of nanotube-based catalysts have been demonstrated in heterogeneous catalysis. Ru-supported nanotubes were found to be superior to the same metal on graphite and on other carbons in the liquid phase hydrogenation reaction of cinnamaldehyde [55]. The properties of catalytically grown carbon nanofibers (which are basically defective nanotubes) have been found to be desirable for high power electrochemical capacitors [56].

## 2.1 Electrochemical Intercalation of Carbon Nanotubes with Lithium

The basic working mechanism of rechargeable lithium batteries is electrochemical intercalation and de-intercalation of lithium between two working electrodes. Current state-of-art lithium batteries use transition metal oxides (i.e.,  $\text{Li}_x\text{CoO}_2$  or  $\text{Li}_x\text{Mn}_2\text{O}_4$ ) as the cathodes and carbon materials (graphite or disordered carbon) as the anodes [57]. It is desirable to have batteries with a high energy capacity, fast charging time and long cycle time. The energy capacity is determined by the saturation lithium concentration of the electrode materials. For graphite, the thermodynamic equilibrium saturation concentration is  $\text{LiC}_6$  which is equivalent to 372 mA h/g. Higher Li concentrations have been reported in disordered carbons (hard and soft carbon) [58,59] and metastable compounds formed under pressure [60].

It has been speculated that a higher Li capacity may be obtained in carbon nanotubes if all the interstitial sites (inter-shell van der Waals spaces, inter-tube channels, and inner cores) are accessible for Li intercalation. Electrochemical intercalation of MWNTs [61,62] and SWNTs [63,64] has been investigated by several groups. Figure 8 (top) shows representative electrochemical intercalation data collected from an arc-discharge-grown MWNT sample using an electrochemical cell with a carbon nanotube film and a lithium foil as the two working electrodes [64]. A reversible capacity ( $C_{\text{rev}}$ ) of 100–640 mA h/g has been reported, depending on the sample processing and annealing conditions [61,62,64]. In general, well-graphitized MWNTs such as those synthesized by the arc-discharge method have a lower  $C_{\text{rev}}$  than those prepared by the CVD method. Structural studies [65,66] have shown that alkali metals can be intercalated into the inter-shell spaces within the individual MWNTs through defect sites.

Single-walled nanotubes are shown to have both high reversible and irreversible capacities [63,64]. Two separate groups reported 400–650 mA h/g reversible and  $\sim 1000$  mA h/g irreversible capacities in SWNTs produced by the

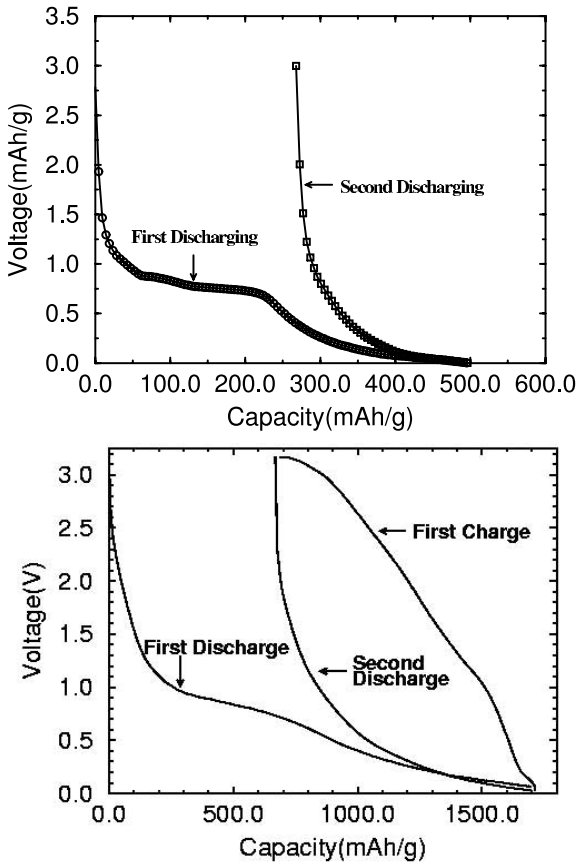


**Fig. 8.** *Top:* Electrochemical intercalation of MWNTs with lithium. Data were collected using 50 mA/h current. The electrolyte was  $\text{LiClO}_4$  in ethylene carbonate/dimethyl carbonate. *Bottom:* Charge-discharge data of purified and processed SWNTs. The reversible capacity of this material is 1000 mA h/g. (Figures are from Gao et al. in [64])

laser ablation method. The exact locations of the Li ions in the intercalated SWNTs are still unknown. Intercalation and *in-situ* TEM and EELS measurements on *individual* SWNT bundles suggested that the intercalants reside in the interstitial sites between the SWNTs [67]. It is shown that the Li/C ratio can be further increased by ball-milling which fractures the SWNTs [68]. A reversible capacity of 1000 mA h/g [64] was reported in processed SWNTs. The large irreversible capacity is related to the large surface area of the SWNT films ( $\sim 300 \text{ m}^2/\text{g}$  by BET characterization) and the formation of a solid-electrolyte-interface. The SWNTs are also found to perform well under high current rates. For example, 60% of the full capacity can be retained when the charge-discharge rate is increased from 50 mA/h to 500 mA/h [63].

The high capacity and high-rate performance warrant further studies on the potential of utilizing carbon nanotubes as battery electrodes. The large observed voltage hysteresis (Fig. 8) is undesirable for battery application. It is at least partially related to the kinetics of the intercalation reaction and can potentially be reduced/eliminated by processing, i.e., cutting the nanotubes to short segments.

## 2.2 Hydrogen Storage

The area of hydrogen storage in carbon nanotubes remains active and controversial. Extraordinarily high and reversible hydrogen adsorption in SWNT-containing materials [69,70,71,72] and graphite nanofibers (GNFs) [73] has been reported and has attracted considerable interest in both academia and industry. Table 2 summarizes the gravimetric hydrogen storage capacity reported by various groups [74]. However, many of these reports have not been independently verified. There is also a lack of understanding of the basic mechanism(s) of hydrogen storage in these materials.

**Table 2.** Summary of reported gravimetric storage of H<sub>2</sub> in various carbon materials (adapted from [74])

Material	Max. wt% H <sub>2</sub>	<i>T</i> (K)	<i>P</i> (MPa)
SWNTs(low purity)	5–10	133	0.040
SWNTs(high purity)	~4	300	0.040
GNFs(tubular)	11.26	298	11.35
GNFs(herringbone)	67.55	298	11.35
GNS(platelet)	53.68	298	11.35
Graphite	4.52	298	11.35
GNFs	0.4	298-773	0.101
Li-GNFs	20	473-673	0.101
Li-Graphites	14	473-674	0.101
K-GNFs	14	<313	0.101
K-Graphite	5.0	<313	0.101
SWNTs(high purity)	8.25	80	7.18
SWNTs(~50% pure)	4.2	300	10.1

Materials with high hydrogen storage capacities are desirable for energy storage applications. Metal hydrides and cryo-adsorption are the two commonly used means to store hydrogen, typically at high pressure and/or low temperature. In metal hydrides, hydrogen is reversibly stored in the interstitial sites of the host lattice. The electrical energy is produced by direct electrochemical conversion. Hydrogen can also be stored in the gas phase in the metal hydrides. The relatively low gravimetric energy density has limited the application of metal hydride batteries. Because of their cylindrical and

hollow geometry, and nanometer-scale diameters, it has been predicted that the carbon nanotubes can store liquid and gas in the inner cores through a capillary effect [76]. A Temperature-Programmed Desorption (TPD) study on SWNT-containing material (0.1–0.2 wt% SWNT) estimates a gravimetric storage density of 5–10 wt% SWNT when H<sub>2</sub> exposures were carried out at 300 torr for 10 min at 277 K followed by 3 min at 133 K [69]. If all the hydrogen molecules are assumed to be inside the nanotubes, the reported density would imply a much higher packing density of H<sub>2</sub> inside the tubes than expected from the normal H<sub>2</sub>–H<sub>2</sub> distance. The same group recently performed experiments on purified SWNTs and found essentially no H<sub>2</sub> adsorption at 300 K [75]. Upon cutting (opening) the nanotubes by an oxidation process, the amount of absorbed H<sub>2</sub> molecules increased to 4–5 wt%. A separate study on higher purity materials reports ~8 wt% of H<sub>2</sub> adsorption at 80 K, but using a much higher pressure of 100 atm [77], suggesting that nanotubes have the highest hydrogen storage capacity of any carbon material. It is believed that hydrogen is first adsorbed on the outer surface of the crystalline ropes.

An even higher hydrogen uptake, up to 14–20 wt%, at 20–400°C under ambient pressure was reported [70] in alkali-metal intercalated carbon nanotubes. It is believed that in the intercalated systems, the alkali metal ions act as a catalytic center for H<sub>2</sub> dissociative adsorption. FTIR measurements show strong alkali–H and C–H stretching modes. An electrochemical absorption and desorption of hydrogen experiment performed on SWNT-containing materials (MER Co, containing a few percent of SWNTs) reported a capacity of 110 mA h/g at low discharge currents [72]. The experiment was done in a half-cell configuration in 6 M KOH electrolyte and using a nickel counter electrode. Experiments have also been performed on SWNTs synthesized by a hydrogen arc-discharge method [71]. Measurements performed on relatively large amount materials (~50% purity, 500 mg) showed a hydrogen storage capacity of 4.2 wt% when the samples were exposed to 10 MPa hydrogen at room temperature. About 80% of the absorbed H<sub>2</sub> could be released at room temperature [71].

The potential of achieving/exceeding the benchmark of 6.5 wt% H<sub>2</sub> to system weight ratio set by the Department of Energy has generated considerable research activities in universities, major automobile companies and national laboratories. At this point it is still not clear whether carbon nanotubes will have real technological applications in the hydrogen storage applications area. The values reported in the literature will need to be verified on well-characterized materials under controlled conditions. What is also lacking is a detailed understanding on the storage mechanism and the effect of materials processing on hydrogen storage. Perhaps the ongoing neutron scattering and proton nuclear magnetic resonance measurements will shed some light in this direction.

In addition to hydrogen, carbon nanotubes readily absorb other gaseous species under ambient conditions which often leads to drastic changes in their

electronic properties[78,79,112]. This environmental sensitivity is a double-edged sword. From the technological point of view, it can potentially be utilized for gas detection[112]. On the other hand, it makes very difficult to deduce the intrinsic properties of the nanotubes, as demonstrated by the recent transport[78] and nuclear magnetic resonance[79] measurements. Care must be taken to remove the adsorbed species which typically requires annealing the nanotubes at elevated temperatures under at least  $10^{-6}$  torr dynamic vacuum.

### 3 Filled Composites

The mechanical behavior of carbon nanotubes is exciting since nanotubes are seen as the “ultimate” carbon fiber ever made. The traditional carbon fibers [17,18] have about *fifty times* the specific strength (strength/density) of steel and are excellent load-bearing reinforcements in composites. Nanotubes should then be ideal candidates for structural applications. Carbon fibers have been used as reinforcements in high strength, light weight, high performance composites; one can typically find these in a range of products ranging from expensive tennis rackets to spacecraft and aircraft body parts. NASA has recently invested large amounts of money in developing carbon nanotube-based composites for applications such as the futuristic Mars mission.

Early theoretical work and recent experiments on individual nanotubes (mostly MWNTs) have confirmed that nanotubes are one of the stiffest structures ever made [81,82,83,84,85]. Since carbon-carbon covalent bonds are one of the strongest in nature, a structure based on a perfect arrangement of these bonds oriented along the axis of nanotubes would produce an exceedingly strong material. Theoretical studies have suggested that SWNTs could have a Young’s modulus as high as 1 TPa [82], which is basically the in-plane value of defect free graphite. For MWNTs, the actual strength in practical situations would be further affected by the sliding of individual graphene cylinders with respect to each other. In fact, very recent experiments have evaluated the tensile strength of individual MWNTs using a nano-stressing stage located within a scanning electron microscope [86]. The nanotubes broke by a sword-in-sheath failure mode [17]. This failure mode corresponds to the sliding of the layers within the concentric MWNT assembly and the breaking of individual cylinders independently. Such failure modes have been observed previously in vapor grown carbon fibers [17]. The observed tensile strength of individual MWNTs corresponded to <60 GPa. Experiments on individual SWNT ropes are in progress and although a sword-in-sheath failure mode cannot occur in SWNT ropes, failure could occur in a very similar fashion. The individual tubes in a rope could pull out by shearing along the rope axis, resulting in the final breakup of the rope, at stresses much below the tensile strength of individual nanotubes. Although testing of individual

nanotubes is challenging, and requires specially designed stages and nano-size loading devices, some clever experiments have provided valuable insights into the mechanical behavior of nanotubes and have provided values for their modulus and strength. For example, in one of the earlier experiments, nanotubes projecting out onto holes in a TEM specimen grid were assumed to be equivalent to clamped homogeneous cantilevers; the horizontal vibrational amplitudes at the tube ends were measured from the blurring of the images of the nanotube tips and were then related to the Young's modulus [83]. Recent experiments have also used atomic force microscopy to bend nanotubes attached to substrates and thus obtain quantitative information about their mechanical properties [84,87].

Most of the experiments done to date corroborate theoretical predictions suggesting the values of Young's modulus of nanotubes to be around 1 TPa (Fig. 9). Although the theoretical estimate for the tensile strength of individual SWNTs is about 300 GPa, the best experimental values (on MWNTs) are close to  $\sim 50$  GPa [86], which is still an order of magnitude higher than that of carbon fibers [17,18].

The fracture and deformation behavior of nanotubes is intriguing. Simulations on SWNTs have suggested very interesting deformation behavior; highly deformed nanotubes were seen to switch reversibly into different morphological patterns with abrupt releases of energy. Nanotubes gets flattened, twisted and buckled as they deform (Fig. 9). They sustain large strains (40%) in tension without showing signs of fracture [82]. The reversibility of deformations, such as buckling, has been recorded directly for MWNT, under TEM observations [7]. Flexibility of MWNTs depends on the number of layers that make up the nanotube walls; tubes with thinner walls tend to twist and flatten more easily. This flexibility is related to the in-plane flexibility of a planar graphene sheet and the ability for the carbon atoms to rehybridize, with the degree of  $sp^2$ - $sp^3$  rehybridization depending on the strain. Such flexibility of nanotubes under mechanical loading is important for their potential application as nanoprobe, for example, for use as tips of scanning probe microscopes.

Recently, an interesting mode of plastic behavior has been predicted in nanotubes [88]. It is suggested that pairs of 5-7 (pentagon-heptagon) pair defects, called a Stone-Wales defect [89], in  $sp^2$  carbon systems, are created at high strains in the nanotube lattice and that these defect pairs become mobile. This leads to a step-wise diameter reduction (localized necking) of the nanotube. These defect pairs become mobile. The separation of the defects creates local necking of the nanotube in the region where the defects have moved. In addition to localized necking, the region also changes lattice orientation (similar in effect to a dislocation passing through a crystal). This extraordinary behavior initiates necking but also introduces changes in helicity in the region where the defects have moved (similar to a change in lattice orientation when a dislocation passes through a crystal). This extraor-

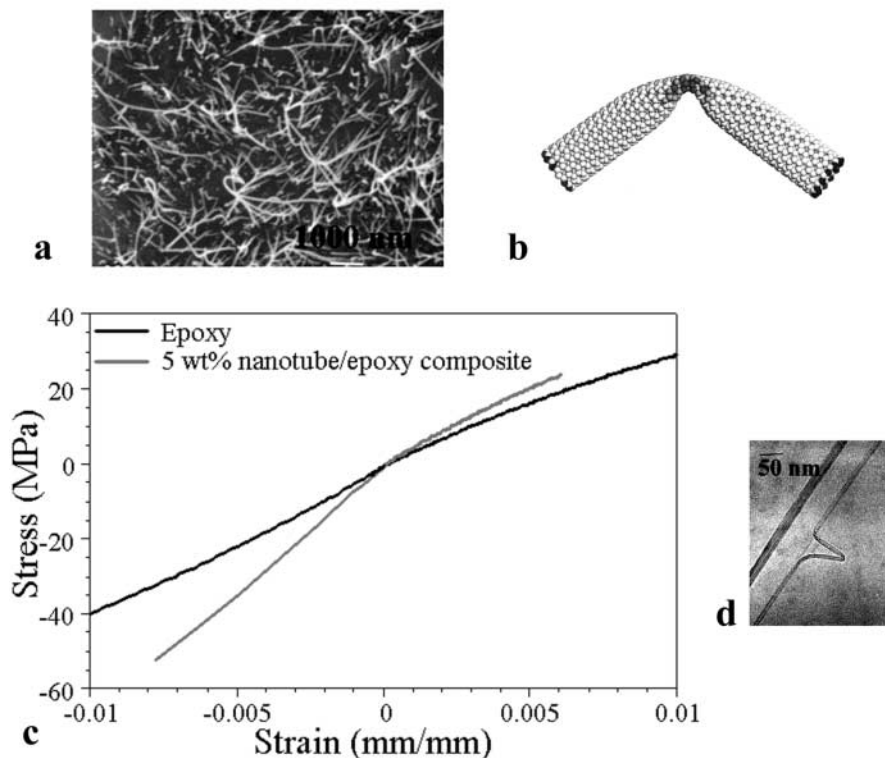


**Fig. 9.** Results of the mechanical properties from MWNT-polymer (epoxy) composites. (a) SEM micrograph that shows good dispersion of MWNTs in the polymer matrix. The tubes are, however, elastically bent due to their highly flexible nature. Schematic of an elastically bent nanotube is shown in (b) (courtesy Prof. Boris Yakobson). The strain is concentrated locally near the bend. (c) Stress-strain relationship observed during the tension/compression testing of the nanotube-epoxy (5 wt% MWNTs) composite (the curve that shows larger slope, both on the tension and compression sides of the stress-strain curve, belongs to the nanotube epoxy composite). It can be seen that the load transfer to the nanotube is higher during the compression cycle (seen from the deviation of the composite curve from that of the pure epoxy), because in tension the individual layers of the nanotubes slide with respect to each other. (d) TEM image of a thicker straight MWNT as well as a buckled MWNT in an epoxy matrix after loading. The smaller diameter nanotubes have more tendency to bend and buckle [86]

dinary behavior could lead to a unique nanotube application: a new type of probe, which responds to mechanical stress by changing its electronic character. High temperature fracture of individual nanotubes under tensile loading, has been studied by molecular dynamics simulations [90]. Elastic stretching elongates the hexagons until, at high strain, some bonds are broken. This

local defect is then redistributed over the entire surface, by bond saturation and surface reconstruction. The final result of this is that instead of fracturing, the nanotube lattice unravels into a linear chain of carbon atoms. Such behavior is extremely unusual in crystals and could play a role in increasing the toughness (by increasing the energy absorbed during deformation) of nanotube-filled ceramic composites during high temperature loading.

The most important application of nanotubes based on their mechanical properties will be as reinforcements in composite materials. Although nanotube-filled polymer composites are an obvious materials application area, there have not been many successful experiments, which show the advantage of using nanotubes as fillers over traditional carbon fibers. The main problem is in creating a good interface between nanotubes and the polymer matrix and attaining good load transfer from the matrix to the nanotubes, during loading. The reason for this is essentially two-fold. First, nanotubes are atomically smooth and have nearly the same diameters and aspect ratios (length/diameter) as polymer chains. Second, nanotubes are almost always organized into aggregates which behave differently in response to a load, as compared to individual nanotubes. There have been conflicting reports on the interface strength in nanotube-polymer composites [91,92,93,94,95,96]. Depending on the polymer used and processing conditions, the measured strength seems to vary. In some cases, fragmentation of the tubes has been observed, which is an indication of a strong interface bonding. In some cases, the effect of sliding of layers of MWNTs and easy pull-out are seen, suggesting poor interface bonding. Micro-Raman spectroscopy has validated the latter, suggesting that sliding of individual layers in MWNTs and *shearing* of individual tubes in SWNT ropes could be limiting factors for good load transfer, which is essential for making high strength composites. To maximize the advantage of nanotubes as reinforcing structures in high strength composites, the aggregates need to be broken up and dispersed or cross-linked to prevent slippage [97]. In addition, the surfaces of nanotubes have to be chemically modified (functionalized) to achieve strong interfaces between the surrounding polymer chains (Fig. 10).

There are certain advantages that have been realized in using carbon nanotubes for structural polymer (e.g., epoxy) composites. Nanotube reinforcements will increase the toughness of the composites by absorbing energy during their highly flexible elastic behavior. This will be especially important for nanotube-based ceramic matrix composites. An increase in fracture toughness on the order of 25% has been seen in nano-crystalline alumina nanotube (5% weight fraction) composites, without compromising on hardness [98]. Other interesting applications of nanotube-filled polymer films will be in adhesives where a decoration of nanotubes on the surface of the polymer films could alter the characteristics of the polymer chains due to interactions between the nanotubes and the polymer chains; the high surface area of the nanotube structures and their dimensions being nearly that of the linear di-

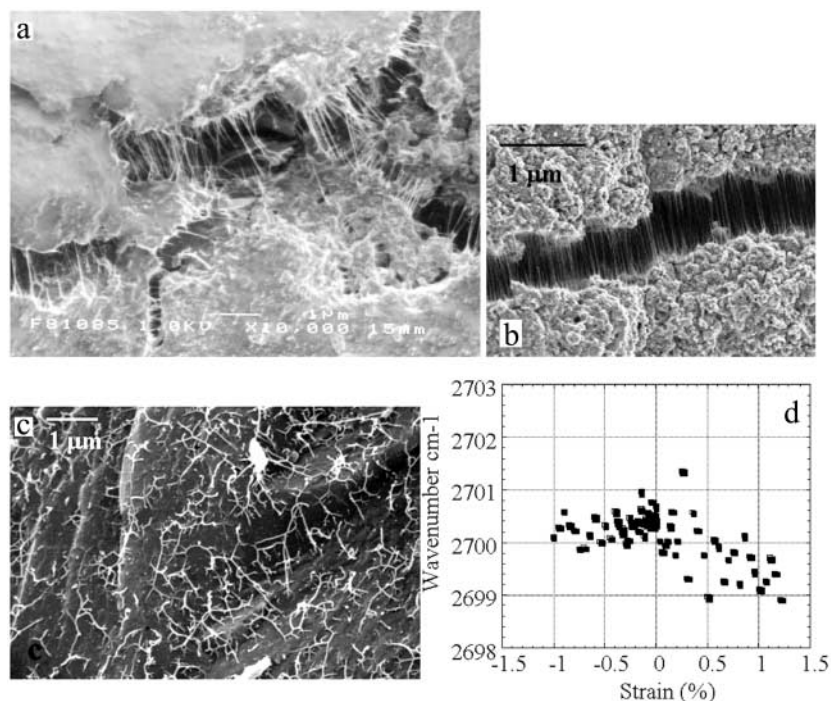


**Fig. 10.** Results of mechanical properties measurements on SWNT-polymer composites. (a) SEM micrograph that shows a partially fractured surface of a SWNT-epoxy composite, indicating stretched nanotubes extending across cracks. (b) Shows a similar event illustrating the stretching and aligning of SWNT bundles across a long crack in a SWNT-carbon soot composite. (c) SEM micrograph that shows the surface of a fractured SWNT-epoxy composite where the nanotube ropes have been completely pulled out and have fallen back on the fractured surface, forming a loose random network of interconnected ropes. (d) Shows results of micro-Raman spectroscopy that detects peak-shifts (in wave-numbers) as a function of strain. In both tension and compression of the SWNT-epoxy specimens, the peak shifts are negligible, suggesting no load transfer to the nanotubes during the loading of the composites [97]

mensions of the polymer chains could give such nanocomposites new surface properties. The low density of the nanotubes will clearly be an advantage for nanotube-based polymer composites, in comparison to short carbon fiber reinforced (random) composites. Nanotubes would also offer multifunctionality, such as increased electrical conduction. Nanotubes will also offer better performance during compressive loading in comparison to traditional carbon fibers due to their flexibility and low propensity for carbon nanotubes to fracture under compressive loads.

Other than for structural composite applications, some of the unique properties of carbon nanotubes are being pursued by filling photo-active polymers with nanotubes. Recently, such a scheme has been demonstrated in a conjugated luminescent polymer, poly(*m*-phenylenevinylene-co-2,5-dioctoxy-*p*-phenylenevinylene) (PPV), filled with MWNTs and SWNTs [99]. Nanotube/PPV composites have shown large increases in electrical conductivity (by nearly eight orders of magnitude) compared to the pristine polymer, with little loss in photoluminescence/electro-luminescence yield. In addition, the composite is far more robust than the pure polymer regarding mechanical strength and photo-bleaching properties (breakdown of the polymer structure due to thermal effects). Preliminary studies indicate that the host polymer interacts weakly with the embedded nanotubes, but that the nanotubes act as nano-metric heat sinks, which prevent the build up of large local heating effects within the polymer matrix. While experimenting with the composites of conjugated polymers, such as PPV and nanotubes, a very interesting phenomenon has been recently observed [80]; it seems that the coiled morphology of the polymer chains helps to wrap around nanotubes suspended in dilute solutions of the polymer. This effect has been used to separate nanotubes from other carbonaceous material present in impure samples. Use of the non-linear optical and optical limiting properties of nanotubes has been reported for designing nanotube-polymer systems for optical applications, including photo-voltaic applications [100]. Functionalization of nanotubes and the doping of chemically modified nanotubes in low concentrations into photo-active polymers, such as PPV, have been shown to provide a means to alter the hole transport mechanism and hence the optical properties of the polymer. Small loadings of nanotubes are used in these polymer systems to tune the color of emission when used in organic light emitting devices [101]. The interesting optical properties of nanotube-based composite systems arise from the low dimensionality and unique electronic band structure of nanotubes; such applications cannot be realized using larger micron-size carbon fibers (Fig. 11).

There are other less-explored areas where nanotube-polymer composites could be useful. For example, nanotube filled polymers could be useful in ElectroMagnetic Induction (EMI) shielding applications where carbon fibers have been used extensively [17]. Membranes for molecular separations (especially biomolecules) could be built from nanotube-polycarbonate systems, making use of the remarkable small pores sizes that exist in nanotubes. Very recently, work done at RPI suggests that composites made from nanotubes (MWNTs) and a biodegradable polymer (polylactic acid; PLA) act more efficiently than carbon fibers for osteointegration (growth of bone cells), especially under electrical stimulation of the composite.

There are challenges to be overcome when processing nanotube composites. One of the biggest problems is dispersion. It is extremely difficult to separate individual nanotubes during mixing with polymers or ceramic ma-

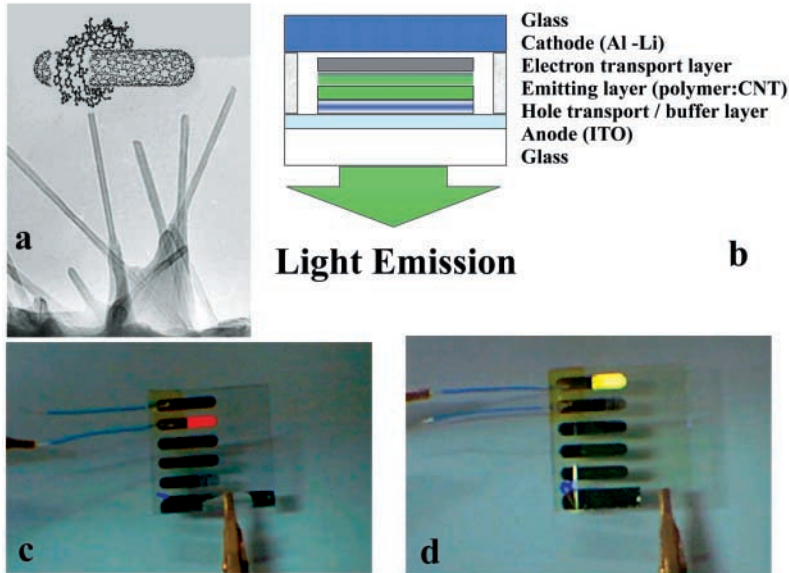


**Fig. 11.** Results from the optical response of nanotube-doped polymers and their use in Organic Light Emitting Diodes (OLED). The construction of the OLED is shown in the schematic of (*top*). The *bottom* figure shows emission from OLED structures. Nanotube doping tunes the emission color. With SWNTs in the buffer layer, holes are blocked and recombination takes place in the transport layer and the emission color is red [101]. Without nanotubes present in the buffer layer, the emission color is green (not shown in the figure) (figures are courtesy of Prof. David Carroll)

materials and this creates poor dispersion and clumping together of nanotubes, resulting in a drastic decrease in the strength of composites. By using high power ultrasound mixers and using surfactants with nanotubes during processing, good nanotube dispersion may be achieved, although the strengths of nanotube composites reported to date have not seen any drastic improvements over high modulus carbon fiber composites. Another problem is the difficulty in fabricating high weight fraction nanotube composites, considering the high surface area for nanotubes which results in a very high viscosity for nanotube-polymer mixtures. Notwithstanding all these drawbacks, it needs to be said that the presence of nanotubes stiffens the matrix (the role is especially crucial at higher temperatures) and could be very useful as a matrix modifier [102], particularly for fabricating improved matrices useful for carbon fiber composites. The real role of nanotubes as an efficient reinforcing fiber will have to wait until we know how to manipulate the nanotube surfaces chemically to make strong interfaces between individual nanotubes (which are really the strongest material ever made) and the matrix materials. In the meanwhile, novel and unconventional uses of nanotubes will have to take the center stage.

## 4 Nanoprobes and Sensors

The small and uniform dimensions of the nanotubes produce some interesting applications. With extremely small sizes, high conductivity, high mechanical strength and flexibility (ability to easily bend elastically), nanotubes may ultimately become indispensable in their use as nanoprobes. One could think of such probes as being used in a variety of applications, such as high resolution imaging, nano-lithography, nanoelectrodes, drug delivery, sensors and field emitters. The possibility of nanotube-based field emitting devices has been already discussed (see Sect. 1). Use of a single MWNT attached to the end of a scanning probe microscope tip for imaging has already been demonstrated (Fig. 12) [104]. Since MWNT tips are conducting, they can be used in STM, AFM instruments as well as other scanning probe instruments, such as an electrostatic force microscope. The advantage of the nanotube tip is its slenderness and the possibility to image features (such as very small, deep surface cracks), which are almost impossible to probe using the larger, blunter etched Si or metal tips. Biological molecules, such as DNA can also be imaged with higher resolution using nanotube tips, compared to conventional STM tips. MWNT and SWNT tips were used in a tapping mode to image biological molecules such as amyloid-b-protofibrils (related to Alzheimer's disease), with resolution never achieved before [105]. In addition, due to the high elasticity of the nanotubes, the tips do not suffer from crashes on contact with the substrates. Any impact will cause buckling of the nanotube, which generally is reversible on retraction of the tip from the substrate. Attaching

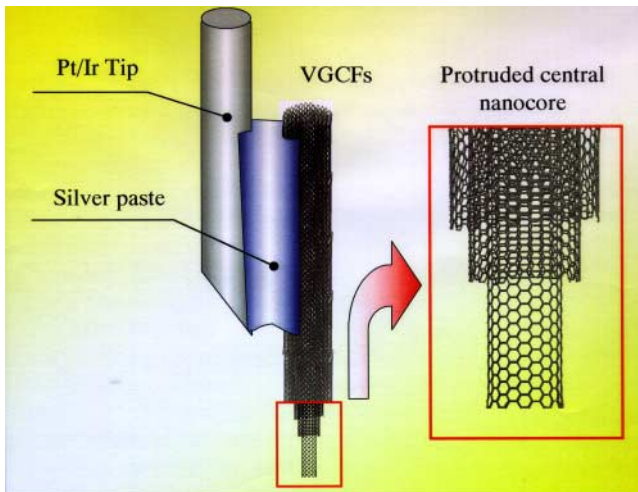


**Fig. 12.** Use of a MWNT as an AFM tip (after *Endo* [103]). At the center of the Vapor Grown Carbon Fiber (VGCF) is a MWNT which forms the tip [18]. The VGCF provides a convenient and robust technique for mounting the MWNT probe for use in a scanning probe instrument

individual nanotubes to the conventional tips of scanning probe microscopes has been the real challenge. Bundles of nanotubes are typically pasted on to AFM tips and the ends are cleaved to expose individual nanotubes (Fig. 12 and also [27]). These tip attachments are not very controllable and will result in vibration problems and in instabilities during imaging, which decrease the image resolution. However, successful attempts have been made to grow individual nanotubes onto Si tips using CVD [106], in which case the nanotubes are firmly anchored to the probe tips. Due to the longitudinal (high aspect) design of nanotubes, nanotube vibration still will remain an issue, unless short segments of nanotubes can be controllably grown (Fig. 12).

In addition to the use of nanotube tips for high resolution imaging, it is also possible to use nanotubes as active tools for surface manipulation. It has been shown that if a pair of nanotubes can be positioned appropriately on an AFM tip, they can be controlled like tweezers to pick up and release nanoscale structures on surfaces; the dual nanotube tip acts as a perfect nano-manipulator in this case [107]. It is also possible to use nanotube tips in AFM nano-lithography. Ten nanometer lines have been written on oxidized silicon substrates using nanotube tips at relatively high speeds [108], a feat that can only be achieved with tips as small as nanotubes.

Since nanotube tips can be selectively modified chemically through the attachment of functional groups [109], nanotubes can also be used as molecular probes, with potential applications in chemistry and biology. Open nanotubes with the attachment of acidic functionalities have been used for chemical and biological discrimination on surfaces [110]. Functionalized nanotubes were used as AFM tips to perform local chemistry, to measure binding forces between protein-ligand pairs and for imaging chemically patterned substrates. These experiments open up a whole range of applications, for example, as probes for drug delivery, molecular recognition, chemically sensitive imaging, and local chemical patterning, based on nanotube tips that can be chemically modified in a variety of ways. The chemical functionalization of nanotubes is a major issue with far-reaching implications. The possibility to manipulate, chemically modify and perhaps polymerize nanotubes in solution will set the stage for nanotube-based molecular engineering and many new nanotechnological applications.

Electromechanical actuators have been constructed using sheets of SWNTs. It was shown that small voltages (a few volts), applied to strips of laminated (with a polymer) nanotube sheets suspended in an electrolyte, bends the sheet to large strains, mimicking the actuator mechanism present in natural muscles [111]. The nanotube actuators would be superior to conducting polymer-based devices, since in the former no ion intercalation (which limits actuator life) is required. This interesting behavior of nanotube sheets in response to an applied voltage suggests several applications, including nanotube-based micro-cantilevers for medical catheter applications and as novel substitutes, especially at higher temperatures, for ferroelectrics.

Recent research has also shown that nanotubes can be used as advanced miniaturized chemical sensors [112]. The electrical resistivities of SWNTs were found to change sensitively on exposure to gaseous ambients containing molecules of  $\text{NO}_2$ ,  $\text{NH}_3$  and  $\text{O}_2$ . By monitoring the change in the conductance of nanotubes, the presence of gases could be precisely monitored. It was seen that the response times of nanotube sensors are at least an order of magnitude faster (a few seconds for a resistance change of one order of magnitude) than those based on presently available solid-state (metal-oxide and polymers) sensors. In addition, the small dimensions and high surface area offer special advantages for nanotube sensors, which could be operated at room temperature or at higher temperatures for sensing applications.

## 5 Templates

Since nanotubes have relatively straight and narrow channels in their cores, it was speculated from the beginning that it might be possible to fill these cavities with foreign materials to fabricate one-dimensional nanowires. Early calculations suggested that strong capillary forces exist in nanotubes, strong enough to hold gases and fluids inside them [113]. The first experimental proof was demonstrated in 1993, by the filling and solidification of molten lead inside the channels of MWNTs [14]. Wires as small as 1.2 nm in diameter were fabricated by this method inside nanotubes. A large body of work now exists in the literature [14,15,16], to cite a few examples, concerning the filling of nanotubes with metallic and ceramic materials. Thus, nanotubes have been used as templates to create nanowires of various compositions and structures (Fig. 13).

The critical issue in the filling of nanotubes is the wetting characteristics of nanotubes, which seem to be quite different from that of planar graphite, because of the curvature of the tubes. Wetting of low melting alloys and solvents occurs quite readily in the internal high curvature pores of MWNTs and SWNTs. In the latter, since the pore sizes are very small, filling is more difficult and can be done only for a selected few compounds. It is intriguing that one could create one-dimensional nanostructures by utilizing the internal one-dimensional cavities of nanotubes. Liquids such as organic solvents wet nanotubes easily and it has been proposed that interesting chemical reactions could be performed inside nanotube cavities [16]. A whole range of experiments remains to be performed inside these constrained one-dimensional spaces, which are accessible once the nanotubes can be opened.

The topology of closed nanotubes provides a fascinating avenue to open them through the simple chemical method of oxidation [114]. As in fullerenes, the pentagonal defects that are concentrated at the tips are more reactive than the hexagonal lattice of the cylindrical parts of the nanotubes. Hence, during oxidation, the caps are removed prior to any damage occurring to the tube body, thus easily creating open nanotubes. The opening of nanotubes

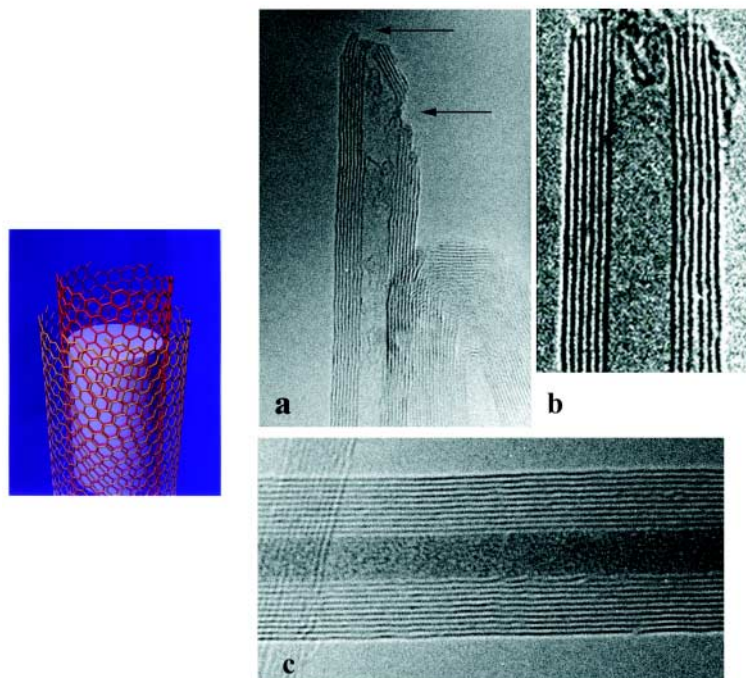


**Fig. 13.** Results that show the use of nanotubes as templates. The *left-hand* figure is a schematic that shows the filling of the empty one-dimensional hollow core of nanotubes with foreign substances. (a) Shows a high-resolution TEM image of a tube tip that has been attacked by oxidation; the preferential attack begins at locations where pentagonal defects were originally present (*arrows*) and serves to open the tube. (b) TEM image that shows a MWNT that has been completely opened by oxidation. (c) TEM image of a MWNT with its cavity filled uniformly with lead oxide. The filling was achieved by capillarity [15]

by oxidation can be achieved by heating nanotubes in air (above 600°C) or in oxidizing solutions (e.g., acids). It is noted here that nanotubes are more stable to oxidation than graphite, as observed in Thermal Gravimetric Analysis (TGA) experiments, because the edge planes of graphite where reaction can initiate are conspicuous by their absence in nanotubes.

After the first set of experiments, reporting the opening and filling of nanotubes in air, simple chemical methods, based on the opening and filling nanotubes in solution, were discovered to develop generalized solution-based strategies to fill nanotubes with a range of materials [15]. In these methods an acid is first used to open the nanotube tip and to act as a low surface tension carrier for solutes (metal-containing salts) to fill the nanotube hollows. Calcination of solvent-treated nanotubes leaves deposits of oxide material (e.g., NiO) inside nanotube cavities. The oxides can then be reduced to metals by

annealing in reducing atmospheres. Observation of solidification inside the one-dimensional channels of nanotubes provides a fascinating study of phase stabilization under geometrical constraints. It is experimentally found that when the channel size gets smaller than a certain critical diameter, solidification results in new and oftentimes disordered phases (e.g.,  $V_2O_5$ ) [115]. Crystalline bulk phases are formed in larger cavities. Numerous modeling studies are under way to understand the solidification behavior of materials inside nanotubes and the physical properties of these unique, filled nano-composite materials.

Filled nanotubes can also be synthesized *in situ*, during the growth of nanotubes in an electric arc or by laser ablation. During the electric arc formation of carbon species, encapsulated nanotubular structures are created in abundance. This technique generally produces encapsulated nanotubes with carbide nanowires (e.g., transition metal carbides) inside [116,117]. Laser ablation also produces heterostructures containing carbon and metallic species. Multi-element nanotube structures consisting of multiple phases (e.g., coaxial nanotube structures containing SiC, SiO, BN and C) have been successfully synthesized by reactive laser ablation [118]. Similarly, post-fabrication treatments can also be used to create heterojunctions between nanotubes and semiconducting carbides [119,120]. It is hoped that these hybrid nanotube-based structures, which are combinations of metallic, semiconducting and insulating nanostructures, will be useful in future nanoscale electronic device applications.

Nanocomposite structures based on carbon nanotubes can also be built by coating nanotubes uniformly with organic or inorganic structures. These unique composites are expected to have interesting mechanical and electrical properties due to a combination of dimensional effects and interface properties. Finely-coated nanotubes with monolayers of layered oxides have been made and characterized (e.g., vanadium pentoxide films) [115]. The interface formed between nanotubes and the layered oxide is atomically flat due to the absence of covalent bonds across the interface. It has been demonstrated that after the coating is made, the nanotubes can be removed by oxidation leaving behind freely-standing nanotubes made of oxides, with nanoscale wall thickness. These novel ceramic tubules, made using nanotubes as templates, could have interesting applications in catalysis. Recently, researchers have also found that nanotubes can be used as templates for the self-assembly of protein molecules [121]. Dipping MWNTs in a solution containing proteins, results in monolayers of proteins covering nanotubes; what is interesting is that the organization of the protein molecules on nanotubes corresponds directly to the helicity of the nanotubes. It seems that nanotubes with controlled helicities could be used as unique probes for molecular recognition, based on the helicity and dimensions, which are recognized by organic molecules of comparable length scales.

There are other ways in which pristine nanotubes can be modified into composite structures. Chemical functionalization can be used to build macromolecular structures from fullerenes and nanotubes. The attachment of organic functional groups on the surface of nanotubes has been achieved, and with the recent success in breaking up SWNTs into shorter fragments, the possibility of functionalizing and building structures through chemistry has become a reality. Decoration of nanotubes with metal particles has been achieved for different purposes, most importantly for use in heterogeneous catalysis [55]. SWNT bundles have been doped with alkali metals, and with the halogens Br<sub>2</sub> and I<sub>2</sub>, resulting in an order of magnitude increase in electrical conductivity [122]. In some cases, it is observed that the dopants form a linear chain and sit in the one-dimensional interstitial channels of the bundles. Similarly, Li intercalation inside nanotubes has been successfully carried out with possible impact on battery applications, which has already been discussed in a previous section. The intercalation and doping studies suggest that nanotube systems provide an effective host lattice for the creation of a range of carbon-based synthetic metallic structures.

The conversion of nanotubes through vapor chemistry can create unique nanocomposites with nanotubes as a backbone. When volatile gases such as halogenated compounds or SiO<sub>x</sub> are reacted with nanotubes, the tubes get converted into carbide nano-rods of similar dimensions [123]. These reactions can be controlled, such that the outer nanotube layers can be converted to carbides, keeping the inner graphite layer structure intact. The carbide rods so produced (e.g., SiC, NbC) should have a wide range of interesting electrical and mechanical properties, which could be exploited for applications as reinforcements and nanoscale electrical devices [124].

## 6 Challenges and Potential for Carbon Nanotube Applications

Carbon nanotubes have come a long way since their discovery in 1991. The structures that were first reported in 1991 were MWNTs with a range of diameters and lengths. These were essentially the distant relatives of the highly defective carbon nanofibers grown via catalytic chemical vapor deposition. The latter types of fibers (e.g., the lower quality carbon nanofibers made commercially by the Hyperion Corporation and more perfect nanotube structures revealed by *Endo* in his 1975 Ph.D. thesis [125]) had existed for more than a decade. The real molecular nanotubes arrived when they were found accidentally while a catalyst (Fe, Co) material was inserted in the anode during electric-arc discharge synthesis. For the first time, there was hope that molecular fibers based purely on carbon could be synthesized and the excitement was tremendous, since many physical properties of such a fiber had already been predicted by theory. It was really the theoretical work proposed

on SWNTs and the availability of nanoscale technology (in characterization and measurements) that made the field take off in 1991.

The greatness of a single-walled nanotube is that it is a macro-molecule and a crystal at the same time. The dimensions correspond to extensions of fullerene molecules and the structure can be reduced to a unit-cell picture, as in the case of perfect crystals. A new predictable (in terms of atomic structure–property relations) carbon fiber was born. The last decade of research has shown that indeed the physical properties of nanotubes are remarkable, as elaborated in the various chapters of this book. A carbon nanotube is an extremely versatile material: it is one of the strongest materials, yet highly elastic, highly conducting, small in size, but stable, and quite robust in most chemically harsh environments. It is hard to think of another material that can compete with nanotubes in versatility.

As a novel material, fullerenes failed to make much of an impact in applications. It seems, from the progress made in recent research, that the story of nanotubes is going to be very different. There are already real products based on nanotubes on the market, for example, the nanotube attached AFM tips used in metrology. The United States, Europe and Japan have all invested heavily in developing nanotube applications. Nanotube-based electronics tops this list and it is comforting that the concepts of devices (such as room-temperature field-effect transistors based on individual nanotubes) have already been successfully demonstrated. As in the case of most products, especially in high technology areas, such as nano-electronics, the time lag between concept demonstration and real products could be several years to decades and one will have to wait and see how long it is going to take nanotube electronics to pervade high technology. Other more obvious and direct applications are some of the bulk uses, such as nanotube-based polymer composites and electrochemical devices. These, although very viable applications, face challenges, as detailed in this review. What is also interesting is that new and novel applications are emerging, as for example, nanotubes affecting the transport of carriers and hence luminescence in polymer-based organic light-emitting diodes, and nanotubes used as actuators in artificial muscles. It can very well be said that some of these newly found uses will have a positive impact on the early stages of nanotube product development.

There are also general challenges that face the development of nanotubes into functional devices and structures. First of all, the growth mechanism of nanotubes, similar to that of fullerenes, has remained a mystery [126]. With this handicap, it is not really possible yet to grow these structures in a controlled way. There have been some successes in growing nanotubes of certain diameter (and to a lesser extent, of predetermined helicity) by tuning the growth conditions by trial and error. Especially for electronic applications, which rely on the electronic structure of nanotubes, this inability to select the size and helicity of nanotubes during growth remains a drawback. More so, many predictions of device applicability are based on joining nano-

tubes via the incorporation of topological defects in their lattices. There is no controllable way, as of yet, of making connections between nanotubes. Some recent reports, however, suggest the possibility of constructing these interconnected structures by electron irradiation and by template mediated growth and manipulation.

For bulk applications, such as fillers in composites, where the atomic structure (helicity) has a much smaller impact on the resulting properties, the quantities of nanotubes that can be manufactured still falls far short of what industry would need. There are no available techniques that can produce nanotubes of reasonable purity and quality in kilogram quantities. The industry would need tonnage quantities of nanotubes for such applications. The market price of nanotubes is also too high presently ( $\sim$ \\$200 per gram) for any realistic commercial application. But it should be noted that the starting prices for carbon fibers and fullerenes were also prohibitively high during their initial stages of development, but have come down significantly in time. In the last 2–3 years, there have been several companies that were set up in the US to produce and market nanotubes. It is hoped that in the next few years nanotubes will be available to consumers for less than US \\$100/pound.

Another challenge is in the manipulation of nanotubes. Nano-technology is in its infancy and the revolution that is unfolding in this field relies strongly on the ability to manipulate structures at the atomic scale. This will remain a major challenge in this field, among several others.

## 7 Conclusions

This review has described several possible applications of carbon nanotubes, with emphasis on materials science-based applications. Hints are made to the electronic applications of nanotubes which are discussed elsewhere [9]. The overwhelming message we would like to convey through this chapter is that the unique structure, topology and dimensions of carbon nanotubes have created a superb all-carbon material, which can be considered as the most perfect fiber that has ever been fabricated. The remarkable physical properties of nanotubes create a host of application possibilities, some derived as an extension of traditional carbon fiber applications, but many are new possibilities, based on the novel electronic and mechanical behavior of nanotubes. It needs to be said that the excitement in this field arises due to the versatility of this material and the possibility to predict properties based on its well-defined perfect crystal lattice. Nanotubes truly bridge the gap between the molecular realm and the macro-world, and are destined to be a star in future technology.

## References

1. H. W. Kroto, J. R. Heath, S. C. O'Brien, S. C. Curl, R. E. Smalley, *Nature* **318**, 162 (1985) [391](#)
2. S. Iijima, *Nature* **354**, 56 (1991) [391](#)
3. M. S. Dresselhaus, G. Dresselhaus, P. C. Eklund, *Science of Fullerenes and Carbon Nanotubes* (Academic, New York 1996) [391](#)
4. T. W. Ebbesen, *Carbon Nanotubes: Preparation and Properties* (CRC, Boca Raton 1997) [391](#)
5. R. Saito, G. Dresselhaus, M. S. Dresselhaus, *Physical Properties of Carbon Nanotubes* (Imperial College Press, London 1998) [391](#)
6. B. I. Yakobson, R. E. Smalley, *American Scientist* **85**, 324 (1997) [391](#)
7. P. M. Ajayan, *Chem. Rev.* **99**, 1787 (1999) [391](#), [407](#)
8. C. Dekker, *Phys. Today*, **22** (May 1999) [391](#), [392](#)
9. S. G. Louie, see chapter in this volume [392](#), [420](#)
10. P. M. Ajayan, T. Ichihashi, S. Iijima, *Chem. Phys. Lett.* **202**, 384 (1993) [392](#)
11. D. L. Carroll, P. Redlich, P. M. Ajayan, J. C. Charlier, X. Blase, A. De Vita, R. Car, *Phys. Rev. Lett.* **78**, 2811 (1997) [392](#)
12. T. W. Ebbesen, P. M. Ajayan, H. Hiura, K. Tanigaki, *Nature* **367**, 519 (1994) [392](#)
13. J. Liu, A. Rinzler, H. Dai, J. Hafner, R. Bradley, P. Boul, A. Lu, T. Iverson, K. Shelimov, C. Huffman, F. Rodriguez-Macias, Y. Shon, R. Lee, D. Colbert, R. E. Smalley, *Science* **280**, 1253 (1998) [392](#)
14. P. M. Ajayan, S. Iijima, *Nature* **361**, 333 (1993) [392](#), [415](#)
15. S. C. Tsang, Y. K. Chen, P. J. F. Harris, M. L. H. Green, *Nature* **372**, 159 (1994) [392](#), [415](#), [416](#)
16. E. Dujardin, T. W. Ebbesen, T. Hiura, K. Tanigaki, *Science* **265**, 1850 (1994) [392](#), [415](#)
17. M. S. Dresselhaus, G. Dresselhaus, K. Sugihara, I. L. Spain, H. A. Goldberg, *Graphite Fibers and Filaments* (Springer, Berlin, Heidelberg 1988) [392](#), [393](#), [406](#), [407](#), [411](#)
18. M. S. Dresselhaus, M. Endo, see chapter in this volume [392](#), [393](#), [406](#), [407](#), [413](#)
19. T. W. Ebbesen, P. M. Ajayan, *Nature* **358**, 220 (1992) [393](#)
20. C. Journet, W. K. Maser, P. Bernier, A. Loiseau, M. Lamy de la Chapelle, S. Lefrant, P. Deniard, R. Lee, J. E. Fischer, *Nature* **388**, 756 (1997) [393](#)
21. A. Thess, R. Lee, P. Nikdaev, H. Dai, P. Petit, J. Robert, C. Xu, Y. H. Lee, S. G. Kim, A. G. Rinzler, D. T. Colbert, G.E. Scuseria, D. Tomanek, J. E. Fischer, R. E. Smalley, *Science* **273**, 483 (1996) [393](#)
22. W. Z. Li, S. S. Xie, L. X. Qian, B. H. Chang, B. S. Zou, W. Y. Zhou, R. A. Zhao, G. Wang, *Science* **274**, 1701 (1996) [393](#)
23. M. Terrones, N. Grobert, J. Olivares, J. P. Zhang, H. Terrones, K. Kordatos, W. K. Hsu, J. P. Hare, P. D. Townshend, K. Prassides, A. K. Cheetham, H. W. Kroto, *Nature* **388**, 52 (1997) [393](#)
24. Z. F. Ren, Z. P. Huang, J. W. Xu, J. H. Wang, P. Bush, M. P. Siegal, P. N. Provencio, *Science* **282**, 1105 (1998) [393](#)
25. J. Kong, H. T. Soh, A. M. Cassell, C. F. Quate, H. Dai, *Nature* **395**, 878 (1998) [393](#)

26. R. Gomer, *Field Emission and Field Ionization* (Harvard Univ. Press, Cambridge, MA 1961) 395
27. L. Forró, C. Schönenberger, see chapter in this volume 395, 414
28. I. Brodie, C. Spindt, *Adv. Electron. Electron Phys.* **83**, 1 (1992) 395
29. J. A. Castellano, *Handbook of Display Technology* (Academic Press, San Diego 1992) 395
30. A. W. Scott, *Understanding Microwaves* (Wiley, New York 1993) 395
31. W. Zhu, G. Kochanski, S. Jin, *Science* **282**, 1471 (1998) 395, 396
32. C. Bower, O. Zhou, W. Zhu, A. G. Ramirez, G. P. Kochanski, S. Jin, in *Amorphous and Nanostructured Carbon*, J. P. Sullivan, J. R. Robertson, B. F. Coll, T. B. Allen, O. Zhou (Eds.) (Mater. Res. Soc.) (in press) 395, 396, 397, 398
33. A. G. Rinzler, J. H. Hafner, P. Nikolaev, L. Lou, S. G. Kim, D. Tomanek, D. Colbert, R. E. Smalley, *Science* **269**, 1550 (1995) 395, 396
34. Y. Saito, K. Hamaguchi, T. Nishino, K. Hata, K. Tohji, A. Kasuya, Y. Nishina, *Jpn. J. Appl. Phys.* **36**, L1340-1342, (1997) 396
35. P. Collins, A. Zettl, *Appl. Phys. Lett.* **69**, 1969 (1996) 396
36. Q. H. Wang, T. D. Corrigan, J. Y. Dai, R. P. H. Chang, A. R. Krauss, *Appl. Phys. Lett.* **70**, 3308 (1997) 396
37. W. de Heer, A. Châtelain, D. Ugarte, *Science* **270**, 1179 (1995) 396
38. O. Kuttel, O. Groening, C. Emmenegger, L. Schlapbach, *Appl. Phys. Lett.* **73**, 2113 (1998) 396
39. J. M. Bonnard, J. P. Salvétat, T. Stockli, W. A. de Herr, L. Forro, A. Chate-lain, *Appl. Phys. Lett.* **73**, 918 (1998) 396
40. W. Zhu, C. Bower, O. Zhou, G. P. Kochanski, S. Jin, *Appl. Phys. Lett.* **75**, 873 (1999) 396, 397
41. K. A. Dean, B. R. Chalamala, *J. Appl. Phys.* **85**, 3832 (1999) 396
42. K. A. Dean, B. R. Chalamala, *Appl. Phys. Lett.* **76**, 375 (2000) 396
43. J. Robertson, *J. Vac. Sci. Technol. B* **17** (1999) 396
44. S. Suzuki, C. Bower, Y. Watanabe, O. Zhou, *Appl. Phys. Lett.* (in press) 396
45. Y. Saito, S. Uemura, K. Hamaguchi, *Jpn. J. Appl. Phys.* **37**, L346 (1998) 398, 399
46. Q. H. Wang, A. A. Setlur, J. M. Lauerhaas, J. Y. Dai, E. W. Seelig, R. H. Chang, *Appl. Phys. Lett.* **72**, 2912 (1998) 399, 400
47. W. B. Choi, D. S. Chung, J. H. Kang, H. Y. Kim, Y. W. Jin, I. T. Han, Y. H. Lee, J. E. Jung, N. S. Lee, G. S. Park, J. M. Kim, *Appl. Phys. Lett.* **75**, 20 (1999) 399
48. R. Standler, *Protection of Electronic Circuits from Over-voltages* (Wiley, New York 1989) 400
49. R. Rosen, W. Simendinger, C. Debbault, H. Shimoda, L. Fleming, B. Stoner, O. Zhou, *Appl. Phys. Lett.* **76**, 1197 (2000) 400, 401
50. R. L. McCreery, *Electroanal. Chem.*, **17**, (ed. A. J. Bard) (Marcel Dekker, New York 1991) 401
51. J. Nugent, K. S. V. Santhanam, A. Rubio, P. M. Ajayan, *J. Phys. Chem.* submitted 401
52. P. J. Britto, K. S. V. Santhanam, P. M. Ajayan, *Bioelectrochem. Bioenergetics* **41**, 121 (1996) 402
53. P. J. Britto, K. S. V. Santhanam, A. Rubio, A. Alonso, P. M. Ajayan, *Adv. Mater.* **11**, 154 (1999) 402
54. G. Che, B. B. Lakshmi, E. R. Fisher, C. R. Martin, *Nature* **393**, 346 (1998) 402

55. J. M. Planeix, N. Coustel, B. Coq, V. Brotons, P. S. Kumbhar, R. Dutartre, P. Geneste, P. Bernier, P. M. Ajayan, *J. Am. Chem. Soc.* **116**, 7935 (1994) [402](#), [418](#)
56. C. Niu, E. K. Sichel, R. Hoch, D. Moy, D. H. Tennet, *Appl. Phys. Lett.* **7**, 1480 (1997) [402](#)
57. M. Whittingham (Ed.), *Recent Advances in Rechargeable Li Batteries*, *Solid State Ionics* **69** (3,4) (1994) [402](#)
58. M. Winter, J. Besenhard, K. Spahr, P. Novak, *Adv. Mater.* **10**, 725 (1998) [402](#)
59. J. R. Dahn, T. Zhang, Y. Liu, J. S. Xue, *Science* **270**, 590(1995) [402](#)
60. V. Avdeev, V. Nalimova, K. Semenenko, *High Pressure Res.* **6**, 11 (1990) [402](#)
61. E. Frackowiak, S. Gautier, H. Gaucher, S. Bonnamy, F. Beguin, *Carbon* **37**, 61 (1999) [402](#)
62. G. T. Wu, C. S. Wang, X. B. Zhang, H. S. Yang, Z. F. Qi, P. M. He, W. Z. Li, *J. Electrochem. Soc.* **146**(5), 1696-1701 (1999) [402](#)
63. A. Claye, R. Lee, Z. Benes, J. Fischer, *J. Electrochem. Soc.* (in press) [402](#), [403](#)
64. B. Gao, A. Kelihammes, X. P. Tang, C. Bower, Y. Wu, O. Zhou, *Chem. Phys. Lett.* **307**, 153 (1999) [402](#), [403](#)
65. O. Zhou, R. M. Fleming, D. W. Murphy, C. T. Chen, R. C. Haddon, A. P. Ramirez, S. H. Glarum, *Science* **263**, 1744 (1994) [402](#)
66. S. Suzuki, M. Tomita, *J. Appl. Phys.* **79**, 3739 (1996) [402](#)
67. S. Suzuki, C. Bower, O. Zhou, *Chem. Phys. Lett.* **285**, 230 (1998) [403](#)
68. B. Gao, C. Bower, O. Zhou (unpublished results) [403](#)
69. A. C. Dillon, K. M. Jones, T. A. Bekkedahl, C. H. Kiang, D. S. Bethune, M. J. Heben, *Nature* **386**, 377 (1997) [404](#), [405](#)
70. P. Chen, X. Wu, J. Lin, K. Tan, *Science* **285**, 91 (1999) [404](#), [405](#)
71. C. Liu, Y. Y. Fan, M. Liu, H. T. Cong, H. M. Cheng, M. S. Dresselhaus, *Science* **286**, 1127 (1999) [404](#), [405](#)
72. C. Nutenadel, A. Zuttel, D. Chartouni, L. Schlapbach, *Solid-State Lett.* **2**, 30 (1999) [404](#), [405](#)
73. A. Chambers, C. Park, R. T. K. Baker, N. M. Rodriguez, *J. Phys. Chem. B* **102**, 4253 (1998) [404](#)
74. M. S. Dresselhaus, K. A. Williams, P. C. Eklund, *MRS Bull.*, **24**, (11), 45 (1999) [404](#)
75. M. J. Heben, Kirchberg (private communication) (2000) [405](#)
76. M. Pederson, J. Broughton, *Phys. Rev. Lett.* **69**, 2689 (1992) [405](#)
77. Y. Ye, C. C. Ahn, C. Witham, B. Fultz, J. Liu, A. G. Rinzler, D. Colbert, K. A. Smith, R. E. Smalley, *Appl. Phys. Lett.* **74**, 2307 (1999) [405](#)
78. P. G. Collins, K. Bradley, M. Ishigami, A. Zettl, *Science*, **287**, 1801-1804 (2000) [406](#)
79. X. P. Tang, A. Kleinhammes, H. Shimoda, L. Fleming, K. Y. Bennoune, C. Bower, O. Zhou, Y. Wu, *Science*, **288**, 492-494 (2000) [406](#)
80. J. N. Coleman, A. B. Dalton, S. Curran, A. Rubio, A. P. Davey, A. Drury, B. McCarthy, B. Lahr, P. M. Ajayan, S. Roth, R. C. Barklie, W. Blau, *Adv. Mater.* **12**, 213 (2000) [411](#)
81. G. Overney, W. Zhong, D. Tomanek, *Z. Phys. D* **27**, 93 (1993) [406](#)
82. B. I. Yakobson, C. J. Brabec, J. Bernholc, *Phys. Rev. Lett.* **76**, 2511 (1996) [406](#), [407](#)

83. M. M. J. Treacy, T. W. Ebbesen, J. M. Gibson, *Nature* **381**, 678 (1996) [406](#), [407](#)
84. E. W. Wong, P. E. Sheehan, C. M. Lieber, *Science* **277**, 1971 (1997) [406](#), [407](#)
85. B. Yakobson, Ph. Avouris, see chapter in this volume. (hoped for chapter) [406](#)
86. M. Yu, O. Lourie, M. J. Dyer, K. Moloni, T. F. Kelly, R. S. Ruoff, *Science* **287**, 637 (2000) [406](#), [407](#), [408](#)
87. M. R. Falvo, C. J. Clary, R. M. Taylor, V. Chi, F. P. Brooks, S. Washburn, R. Superfine, *Nature* **389**, 582 (1997) [407](#)
88. B. I. Yakobson, *Appl. Phys. Lett.* **72**, 918 (1998) [407](#)
89. A. J. Stone, D. J. Wales, *Chem. Phys. Lett.* **128**, 501 (1986) [407](#)
90. B. I. Yakobson, C. J. Brabec, J. Bernholc, *J. Computer Aided Materials Design* **3**, 173 (1996) [408](#)
91. P. M. Ajayan, O. Stephan, C. Colliex, D. Trauth, *Science* **265**, 1212 (1994) [409](#)
92. H. D. Wagner, O. Lourie, Y. Feldman, R. Tenne, *Appl. Phys. Lett.* **72**, 188 (1998) [409](#)
93. L. Jin, C. Bower, O. Zhou, *Appl. Phys. Lett.* **73**, 1197 (1998) [409](#)
94. L. S. Schadler, S. C. Giannaris, P. M. Ajayan, *Appl. Phys. Lett.* **73**, 26 (1999) [409](#)
95. C. Bower, R. Rosen, L. Jin, J. Han, O. Zhou, *Appl. Phys. Lett.* **74**, 3317 (1999) [409](#)
96. P. Calvert, *Nature* **399**, 210 (1999) [409](#)
97. P. M. Ajayan, L. S. Schadler, C. Giannaris, A. Rubio, *Adv. Mater.* (in press) [409](#), [410](#)
98. S. Chang, R. H. Doremus, P. M. Ajayan, R. W. Siegel, unpublished results [409](#)
99. S. Curran, P. M. Ajayan, W. Blau, D. L. Carroll, J. Coleman, A. B. Dalton, A. P. Davey, B. McCarthy, A. Strevens, *Adv. Mater.* **10**, 1091 (1998) [411](#)
100. H. Ago, K. Petritsch, M. S. P. Shaffer, A. H. Windle, R. H. Friend, *Adv. Mater.* **11**, 1281 (1999) [411](#)
101. D. L. Carroll, unpublished results [411](#), [412](#)
102. M. S. P. Shaffer, A. H. Windle, *Adv. Mater.* **11**, 937 (1999) [412](#)
103. M. Endo, unpublished results [413](#)
104. H. J. Dai, J. H. Hafner, A. G. Rinzler, D. T. Colbert, R. E. Smalley, *Nature* **384**, 147 (1996) [413](#)
105. S. S. Wong, J. D. Harper, P. T. Lansbury C. M. Lieber, *J. Am. Chem. Soc.* **120**, 603 (1998) [413](#)
106. J. H. Hafner, C. L. Cheung, C. M. Lieber, *Nature* **398**, 761 (1999) [414](#)
107. P. Kim, C. M. Lieber, *Science* **286**, 2148 (1999) [414](#)
108. S. S. Wong, A. T. Woolley, T. W. Odom, J. L. Huang, P. Kim, D. Vezenov, C. Lieber, *Appl. Phys. Lett.* **73**, 3465 (1998) [414](#)
109. J. Chen, M. Hamon, H. Hu, Y. Chen, A. Rao, P. C. Eklund, R. C. Haddon, *Science* **282**, 95 (1998) [414](#)
110. S. S. Wong, E. Joselevich, A. T. Woolley, C. L. Cheung, C. M. Lieber, *Nature* **394** (1998) [414](#)
111. R. H. Baughman, C. Cui, A. A. Zhakhidov, Z. Iqbal, J. N. Barisci, G. M. Spinks, G. G. Wallace, A. Mazzoldi, D. D. Rossi, A. G. Rinzler, O. Jaschinski, S. Roth, M. Kertesz, *Science* **284**, 1340 (1999) [414](#)

112. J. Kong, N. R. Franklin, C. Zhou, M. C. Chapline, S. Peng, K. Cho, H. Dai, *Science* **287**, 622 (2000) 406, 415
113. M. R. Pederson, J. Q. Broughton, *Phys. Rev. Lett.* **69**, 2689 (1992) 415
114. P. M. Ajayan, T. W. Ebbesen, T. Ichihashi, S. Iijima, K. Tanigaki, H. Hiura, *Nature* **362**, 522 (1993) 415
115. P. M. Ajayan, O. Stephan, P. Redlich, C. Colliex, *Nature* **375**, 564 (1995) 417
116. R. S. Ruoff, D. C. Lorents, B. Chan, R. Malhotra, S. Subramoney, *Science* **259**, 346 (1992) 417
117. C. Guerret-Plecourt, Y. Le Bouar, A. Loiseau, H. Pascard, *Nature* **372**, 761 (1994) 417
118. Y. Zhang, K. Suenaga, C. Colliex, S. Iijima, *Science* **281**, 973 (1998) 417
119. J. Hu, M. Ouyang, P. Yang, C. M. Lieber, *Nature* **399**, 48 (1999) 417
120. Y. Zhang, T. Ichihashi, E. Landree, F. Nihey, S. Iijima, *Science* **285**, 1719 (1999) 417
121. F. Balavoine, P. Schultz, C. Richard, V. Mallouh, T. W. Ebbesen, C. Mioskowski, *Angew. Chem.* **111**, 2036 (1999) 417
122. R. S. Lee, H. J. Kim, J. E. Fischer, A. Thess, R. E. Smalley, *Nature* **388**, 255 (1997) 418
123. H. J. Dai, E. W. Wong, Y. Z. Lu, S. S. Fan, C. M. Lieber, *Nature* **375**, 769 (1995) 418
124. R. Tenne, A. Zettl, see chapter in this volume 418
125. M. Endo, Ph.D. Thesis (1975) 418
126. J. C. Charlier, S. Iijima, see chapter in this volume 419